ELSEVIER

Ceramics International 28 (2002) 51–58

CERAMICS INTERNATIONAL

www.elsevier.com/locate/ceramint

Low temperature hot-pressed BAS matrix composites reinforced with in situ grown Si_3N_4 whiskers

S. Chen[a,b,*], F. Ye[a], Y. Zhou[a]

[a]*School of Materials Science and Engineering, PO Box 433, Harbin Institute of Technology, Harbin 150001, PR China*
[b]*Department of Materials Science and Engineering, Tsinghua University, Beijing 100084, PR China*

Received 25 February 2001; received in revised form 7 March 2001; accepted 22 April 2001

Abstract

A series of Si_3N_4/BAS compositions of 20, 40, 60, 80 and 100 wt.% barium aluminosilicate (BAS) were hot-pressed at relatively low sintering temperature (1450 °) for a 30–60 min soak at a pressure of 10–20 MPa under N_2 atmosphere. Elongated rod-like β-Si_3N_4 whiskers were formed for compositions with 20–80 wt.% BAS. No metal ions were dissolved in Si_3N_4 crystal lattices. The microstructure varied with composition. The relative content of rod-like β-Si_3N_4 whiskers increased with increasing BAS content. Densities of all the specimens with BAS contents more than 20 wt.% were >99% of the theoretical density. With a 30 min soak, the room temperature (RT) flexural strength increased from 259.1 to 323.0 MPa from 20 to 40 wt.% BAS and then decreased to 70.6 MPa for 100 wt.% BAS. The fracture toughness increased from 2.40 to 3.24 MPa $m^{1/2}$ from 20 to 60 wt.% BAS and then decreased to 1.78 MPa $m^{1/2}$ for 100 wt.% BAS. With a 60 min soak, the RT flexural strength of 40 wt.% BAS without monoclinic BAS seeds was 379.6 MPa and retained 87.9, 93.8 and 94.2% of their RT values at 1000, 1100 and 1200 °C, respectively; in contrast, the RT flexural strength of 40 wt% BAS containing 8 wt% BAS seeds was 519.4 MPa and retained 87.3, 63.0 and 51.9% of their RT values at 1000, 1100 and 1200 °C, respectively. Monoclinic BAS seeds had little effect in accelerating the hexagonal→monoclinic phase transformation of BAS glass ceramics.

Keywords: A. Hot pressing; B. Composites; B. Whiskers; C. Mechanical properties; D. Glass-ceramics; D. Si_3N_4

1. Introduction

Low-cost ceramic composite materials that exhibit high strength and toughness, high thermal shock resistance, and good oxidation resistance are attracting considerable interest for emerging high-temperature advanced engineering applications. Glass-ceramics are of particular interest because of their high melting temperature, low thermal expansion, good oxidation resistance and low dielectric constant.

Barium aluminosilicate (BAS) has one of the highest melting temperatures (1760 °C) among the glass-ceramic materials [1] and the monoclinic form exhibits a low thermal expansion coefficient (2.29×10^{-6} °C^{-1} from 22 to 1000 °C) [2]. Therefore, BAS is attracting considerable interest for various applications such as structural and electronic components as well as matrix for ceramic-matrix composites. However, the pure BAS glass-ceramic matrices exhibit relatively low mechanical properties, which limit its use in many structural applications. Ceramic whiskers have been used to reinforce glass-ceramics, resulting in strong, tough and high refractory ceramic composites [3–10]. However, problems associated with fabricating whisker-reinforced ceramic composites include the high cost of whiskers, potential human health hazards in their handling, and processing difficulties such as deagglomeration, mixing, and settling [11,12]. The reports about BAS glass-ceramic matrix composites are limited. Many researchers focused their efforts on lithium aluminosilicate (LAS) glass-ceramic matrix composites [4–6,9,13,14]. But the mechanical properties of LAS matrix composites at 1100 °C decrease greatly compared to the room properties [9,13].

The objectives of this work were to study the microstructure and mechanical behavior of low temperature (1450 °C) hot-pressed BAS matrix composites reinforced with in situ grown Si_3N_4 whiskers. The phase

* Corresponding author.

0272-8842/02/$22.00
PII: S0272-8842(01)00057-8

constitutions, microstructure and whisker/matrix interfacial structures were investigated by means of XRD, EDS, SEM and TEM techniques. The relationships between compositions, holding time and room and elevated temperature mechanical properties were discussed. The strengthening and toughening mechanisms were also discussed.

2. Experimental procedure

The composites used in this study were prepared by BAS glass-ceramic powders and α-Si_3N_4 powders (<5wt.% β-Si_3N_4 existing in the α-Si_3N_4 starting powders). The BAS matrix powders were synthesized through hydrolysis of alkoxides [15]. The XRD patterns of amorphous BAS glass-ceramic and original Si_3N_4 powders are shown in Figs. 1 and 2, respectively. The SEM photographs and chemical compositions of the two original powders are shown in Fig. 3 and Table 1, respectively. In order to study the seeding effect on phase transformation of celsian BAS to hexagonal BAS, monoclinic BAS seeds were added to the composites. The preparation procedure of the monoclinic BAS seeds (particle size: 2–3 μm) is schematically shown in Fig. 4 [16].

The α-Si_3N_4 powders used in this study (supplied by Shanghai Institute of Ceramics, China) had a mean particle diameter of 0.5–1.0 μm. Appropriate proportions of the glass-ceramic powders and α-Si_3N_4 powders were mechanically mixed by ball-milling method in ethyl alcohol using ZrO_2 balls. After milling, the mixture was dried and aggregates were dispersed as required. The dried blends were then hot-pressed in graphite resistance-heated furnace for 30–60 min at 1450 °C in nitrogen atmosphere. The heating and cooling rates ranged from 10 to 30 °C min^{-1}. The composite density was measured by the Archimedes' method.

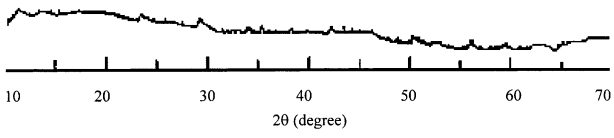

Fig. 1. XRD pattern of sol-gel processed BAS glass ceramic.

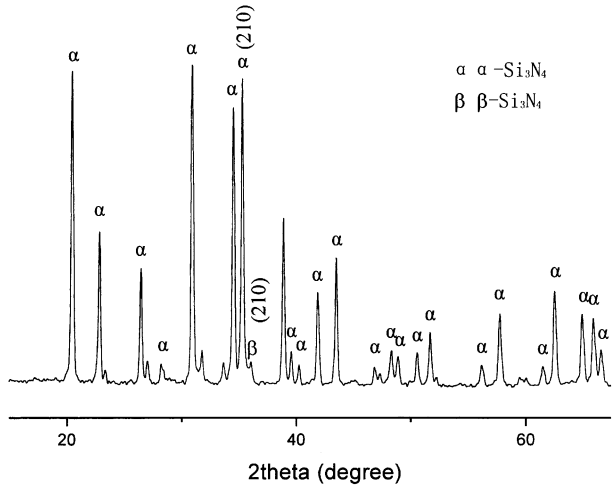

Fig. 2. XRD pattern of original Si_3N_4 powders.

Flexural strength was measured over a temperature range from 25 to 1200 °C in air. All flexural bars were machined with the tensile surface perpendicular to the hot-pressing direction. Flexural strength measurements were performed on bar specimens (3×4×36 mm) using a three-point bending fixture with a span of 30 mm. Elevated-temperature test specimens were introduced to a preheated test chamber and remained 20 min at temperature prior to testing. Fracture toughness was measured in air at 25 °C, performed on single-edge-notched beam specimens (SENB) with a span of 16 mm and a half-thickness notch made by using a 0.33 mm-thick diamond-wafery blade. Six fracture strength and fracture toughness measurements were made for each test condition.

Fracture surfaces of the composites were examined using HITACHI S-570 scanning electron microcope (SEM). Etching of the polished specimens was achieved using HF (5 ml HF, 95 ml H_2O). The SEM specimens were coated with evaporated gold. The phase content was determined by X-ray diffraction (XRD) using CuK_α radiation at an accelerating voltage of 40 kV and a current of 25 mA. The scanning rate was 0.01°/min with a 0.2° detector slit and a 1.0° beam slit. A rotating powder sample holder was used to minimize preferred orientation effects. The microstructural observations and analyses were carried out in a Philips CM-12 transmission electron microscope (TEM) fitted with an energy dispersive X-ray spectrometer (EDS). Thin foil specimens taken normal to the hot-pressing axis were prepared by diamond cutting, grinding and polishing to produce 60 μm thick discs. The resulting disks were then dimpled using standard TEM specimen preparation techniques. The final thinning was accomplished by ion-milling on a cold stage with 4 kV argon ions at incidence angles of 15, 10 and 8°.

3. Results and discussion

3.1. Microstructural characterization

Composites with 20–100 wt.% BAS glass ceramics are densified to 99% of theoretical density. SEM and TEM observations indicate that the distribution of rod-like β-Si_3N_4 whiskers is homogeneous with a preferred long-axes orientation perpendicular to the hot-pressing direction, as shown in Fig. 5. Fig. 5(a) is the fractograph of 60 wt.% BAS composites in which the in situ grown

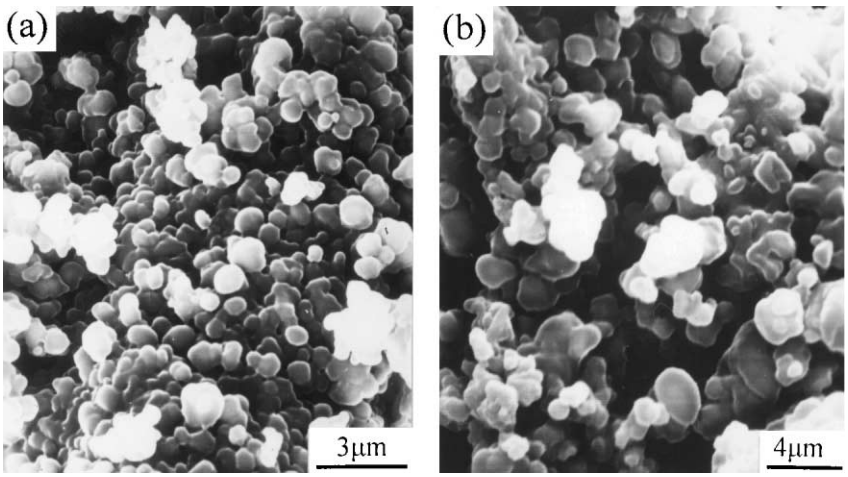

Fig. 3. SEM photographs of original powders: (a) α-Si_3N_4 powders; (b) BAS glass ceramics from sol-gel process.

Table 1
Chemical compositions of BAS matrix and Si_3N_4 powders (wt.%)

Composition content					
BAS			Si_3N_4		
BaO	Al_2O_3	SiO_2	α-Si_3N_4	β-Si_3N_4	Impurities
37	26	37	95.40	3.77	0.83

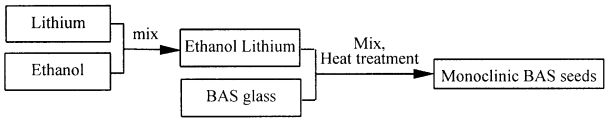

Fig. 4. Flow diagram of the synthesis procedure of the monoclinic BAS seeds [15].

rod-like Si_3N_4 whiskers array perpendicular to the hot-pressing direction, while Fig. 5(b) is the TEM photograph in which the Si_3N_4 whiskers emerging and growing from the Si_3N_4–BAS grain boundary array vertical to the hot-pressing direction.

XRD results of the composites are summarized in Fig. 6 and Table 2. To estimate the amount of α-Si_3N_4 phases, the modified XRD intensities of α- and β-silicon nitride (210) diffraction peaks are compared, in a manner described by Gazzara and Messier[17]. Quantitative analyses of hexacelsian and celsian contents were carried out by comparing the intensity ratios from the (102) plane for hexacelsian with the ($\bar{1}$12) plane for celsian based on the work of Freitag [18]. Three phases were found in the materials without adding monoclinic BAS seeds, including untransformed α-Si_3N_4, β-Si_3N_4 and hexacelsian $BaAl_2Si_2O_8$. Neither orthorhombic BAS nor monoclinic BAS were detected by XRD. From these calculations follows that approximately 27.0–61.6% β-Si_3N_4 formed during sintering. The existence of BAS glass-ceramic could significantly accelerate the formation of rod-like β-Si_3N_4 whiskers. In the sample

Table 2
Summary of XRD analyses of Si_3N_4/BAS composites

Material	XRD phases
BAS	Hexacelsian BAS
Si_3N_4/BAS	α-Si_3N_4, β-Si_3N_4, Hexacelsian
BAS seeds + Si_3N_4/BAS	Hexacelsian, α-Si_3N_4, β-Si_3N_4, Celisan

containing added 20 wt.% monoclinic BAS seeds, only 2.4% hexacelsian BAS transformed to celsian BAS. This indicates that celsian seeds had little effect on the phase transformation at such a low sintering temperature.

The results of TEM observations indicated that the BAS matrix consists mainly of hexacelsian phase, which is consistent with the results of XRD. The microstructures of the composites with 40 and 60 wt.% BAS are shown in Figs. 7 and 8, respectively. Fig. 7(a) reveals that there are quite a number of untransformed equiaxed α-Si_3N_4 grains dispersed in the BAS matrix. Some Si_3N_4 particles that are undergoing α→β-Si_3N_4 phase transformation are also observed [Fig. 7(b)]. The α→β-Si_3N_4 phase transformation is of a reconstructive nature via a solution-reprecipitation mechanism. The nucleation and growth rate of β-Si_3N_4 grains are a function of the rate of dissolution of α-Si_3N_4 particles, solubility of α-Si_3N_4 into the liquid, supersaturation of Si and N in the liquid, interfacial tension and wetting between the silicon nitride grains and liquid, and viscosity of the liquid. The chemistry of the liquid phase is, therefore, a key factor in determining the resulting microstructure and the associated properties of the materials. At the sintering temperature between 1100 and 1450 °C and under the pressure of 10–30 MPa, the BAS glass became soft and partially melting, through which the Si and N can be transferred. Fig. 8 shows that equiaxed α-Si_3N_4 and rod-like β-Si_3N_4 whiskers coexist

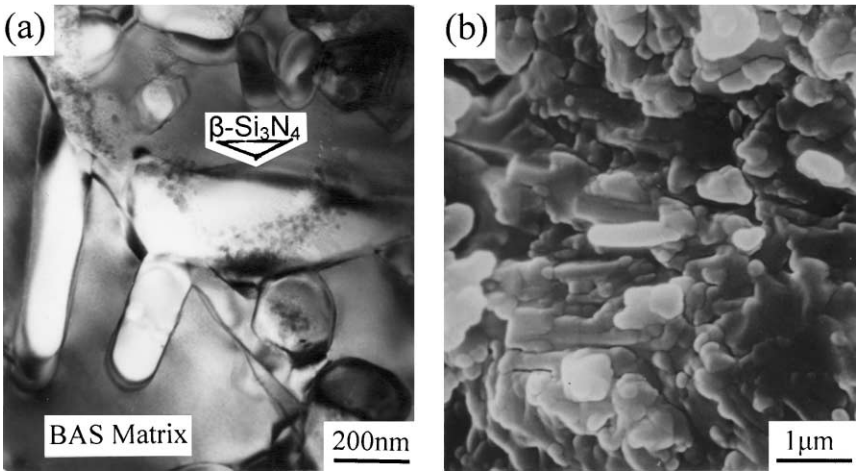

Fig. 5. In situ grown rod-like β-Si_3N_4 whisker orientation in: (a) plane vertical to hot-pressing direction; (b) plane parallel to hot-pressing direction.

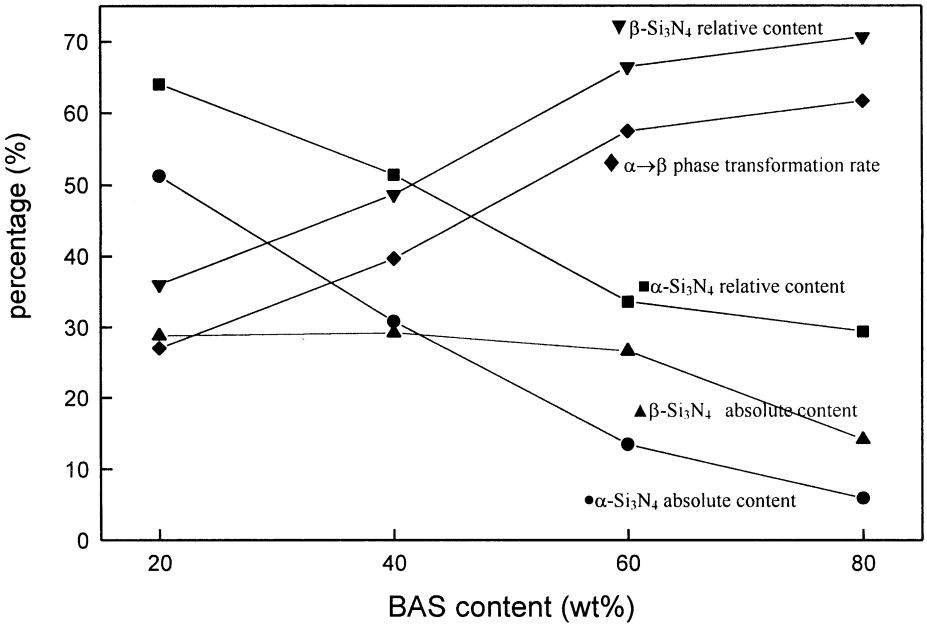

Fig. 6. α→β-Si_3N_4 phase transformation rates as a function of BAS content.

in the BAS matrix. The relative amount of β-Si_3N_4 in the 60 wt.% BAS (66.4%) composites is greater than that in the 40 wt.% BAS composites (48.6%). This corresponds well with the calculated result of the XRD analysis.

β-Si_3N_4 has an extensive solid solubility with Al_2O_3 [19]. Significant dissolution of Al_2O_3 into β-Si_3N_4 may shift the composition of BAS away from the stoichiometric composition. This may increase the amount of residual glass phase. EDS analysis of the whisker areas revealed no substitution of silicon or nitrogen in the Si_3N_4 structure by metal ions, as shown in Fig. 9. This indicates that no Si–Al–O–N composition is formed during low temperature processing.

3.2. Mechanical properties of Si_3N_4/BAS composites

The room temperature flexural strengths of Si_3N_4/BAS composites are shown in Fig. 10 and Table 3. It can be seen that the highest flexural strength of the composites (holding time: 30 min) is obtained for the sample which contains 40 wt.% BAS. The room temperature flexural strength of pure BAS matrix is only 70.4 MPa. The strengths of the composites increase by 145–357% compared to the matrix, indicating that in situ grown rod-like β-Si_3N_4 whiskers provide good strengthening effect. Samples with higher BAS content show a drop in the flexural strength. Table 3 shows that with increasing sintering time and addition of BAS

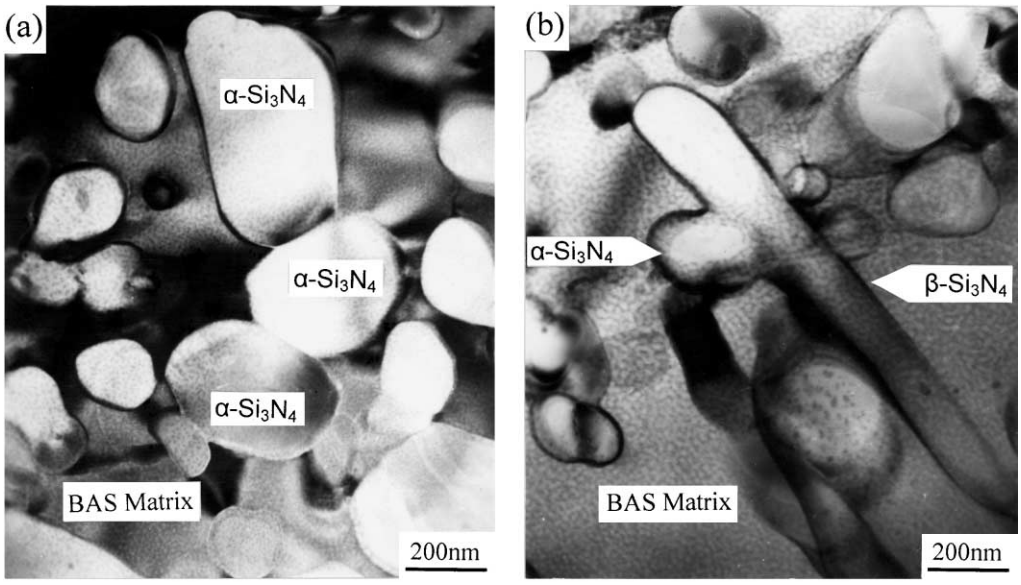

Fig. 7. TEM photographs of 40 wt.% BAS composites: (a) TEM micrograph showing equiaxed α-Si_3N_4 grains in BAS matrix; (b) Si_3N_4 grains undergoing α→β phase transformation.

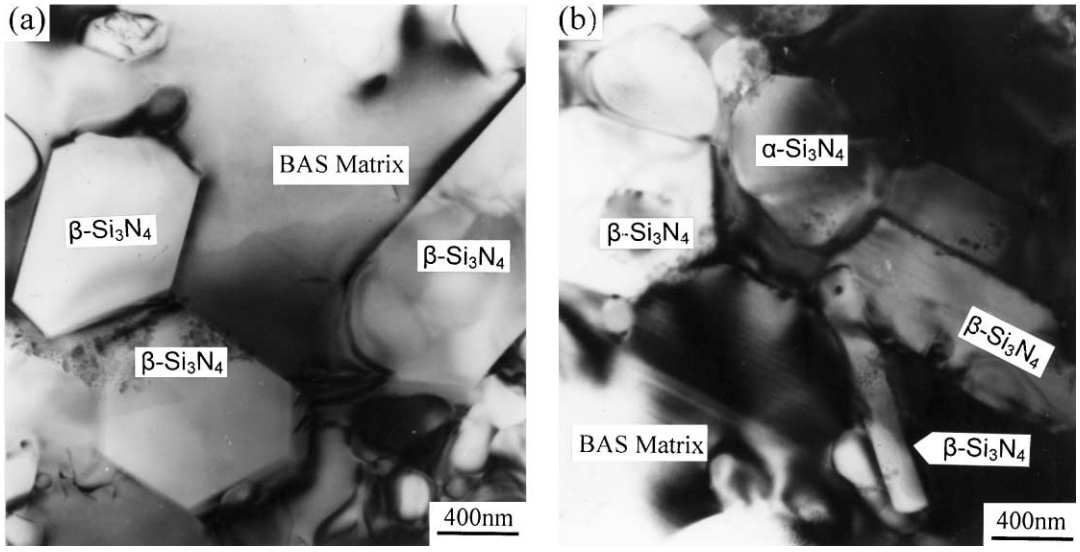

Fig. 8. TEM photographs of 60 wt.% BAS composites: (a) TEM micrograph showing in situ β-Si_3N_4 in the matrix; (b) showing the presence of both α-Si_3N_4 and β-Si_3N_4 in the BAS matrix.

monoclinic BAS seeds, the flexural strengths of 40 wt.% BAS composites increase 17 and 61%, respectively.

As usual, the increase in the strength is contributed to the load transmitting effect from matrix to β-Si_3N_4 whisker. It is typical of liquid-phase sintered silicon nitride materials prepared by dry pressing powders [20]. The relatively low mechanical properties are also due in part to the residual stresses generated by the large difference in thermal expansion between Si_3N_4 (3.0×10^{-6} $^{\circ}C^{-1}$) and hexacelsian (8.0×10^{-6} $^{\circ}C^{-1}$) which develop on cooling from high processing temperatures, the matrix is in tension condition, which would cause cracking in the matrix and hence be harmful to the strength of composite. The observed β-Si_3N_4 whisker strengthening of the composite may be due to the combined effects stated above. Lengthening sintering time will be beneficial to the α→β phase transformation of Si_3N_4, thus increase the mechanical properties. The addition of monoclinic BAS seeds will supply crystal centers during the crystallizing process of BAS and Si_3N_4. It will also weaken the thermal mismatch to some extent. Though the monoclinic BAS seeds could do little effect in accelerating the α→β-Si_3N_4 phase transformation, they could increase the room temperature flexural strength effectively.

The flexural strength of Si_3N_4/BAS composite (40 wt.% BAS) as a function of temperature is shown in

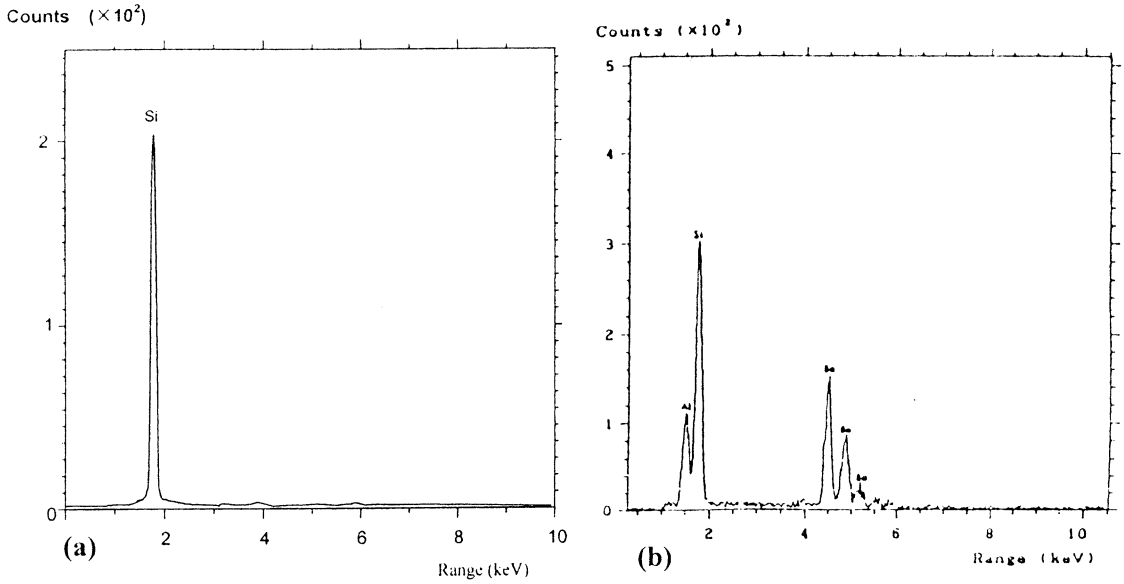

Fig. 9. EDS analysis of BAS matrix and in situ grown β-Si_3N_4 whisker areas; (a) EDS analysis of BAS matrix; (b) EDS analysis of Si_3N_4 showing no substitution of silicon or nitrogen in the Si_3N_4 structure by metal ions.

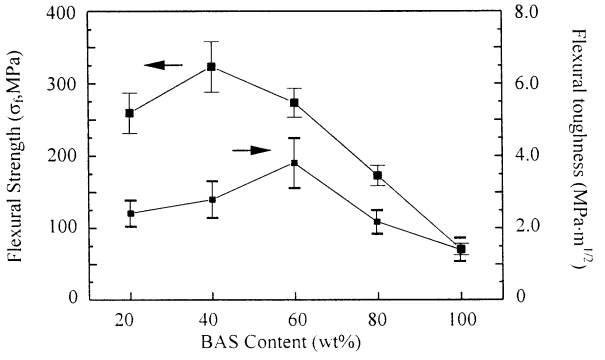

Fig. 10. Flexural strengths of Si_3N_4/BAS composites at room temperature as a function of BAS content (holding time: 30 min).

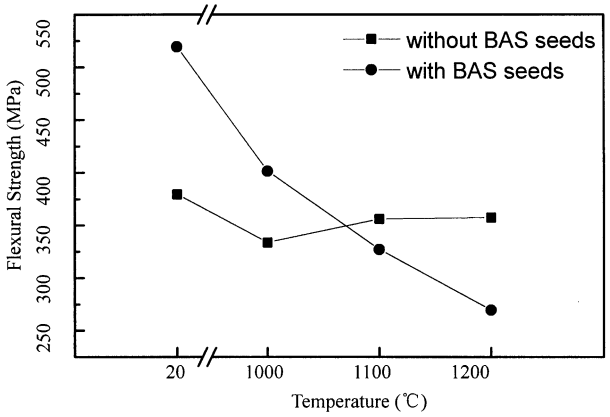

Fig. 11. Flexural strength of Si_3N_4/BAS composite (40 wt.% BAS) as a function of temperature.

Table 3
Room temperature mechanical properties of Si_3N_4/BAS composites

Composite	Flexural strength (MPa)	Fracture toughness (MPa m$^{1/2}$)
40 wt.% BAS, 30 min	323.01±11	2.63±0.31
40 wt.% BAS, 60 min	379.60±15	4.11±0.35
40 wt.% BAS, (containing 20 wt.% seeds), 60 min	519.43±23	5.10±0.40

Fig. 11. Also presented are data for the composites containing 8 wt.% monoclinic BAS seeds. As a result of the seeding effect, the flexural strength of the composite containing BAS seeds is greater than that of non-seed composites at room temperature. At elevated temperatures, however, the strengths of the composite without BAS seeds decreased more slowly. The flexural strength of the composites with and without seeds decreased by 48.1 and 5.84%, respectively. The fractographs of the composites after elevated temperature bending test are shown in Fig. 12. Oxidation pores are observed in the fractograph which indicated oxidizing of Si_3N_4 at elevated temperature. Postset analysis showed that the typical fracture originally occurred at oxidized pores on the order of 2 μm and/or machining flaws on the tensile side of the bars. The drop of strength indicated that the composites might contain amorphous intergranular phase. Although no amorphous phase has been observed during TEM analysis, these data imply the presence of thin films of an amorphous phase adjacent to the silicon nitride grains having dimensions undetectable by conventional TEM. On the other hand, during the fabrication of monoclinic BAS seeds, Li and its compounds are formed. At elevated temperature, the

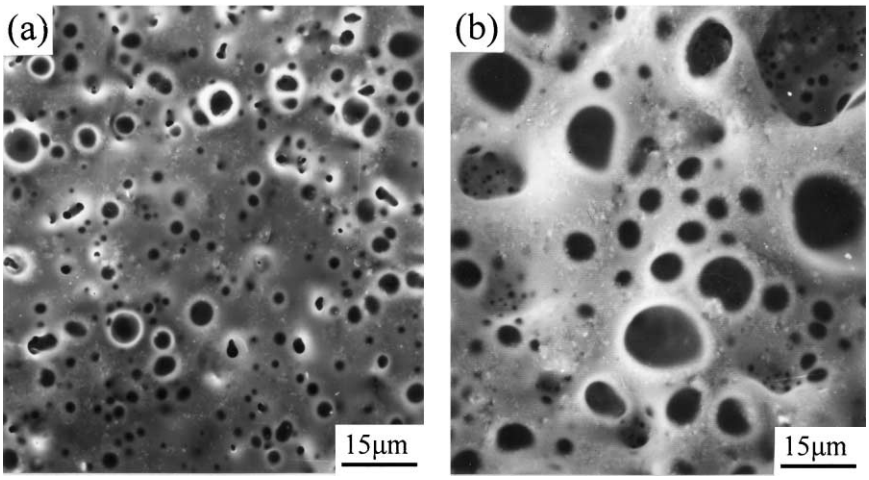

Fig. 12. Fractographs of the composites after elevated temperature bending test (a) 40 wt.% BAS; (b) 60 wt.% BAS.

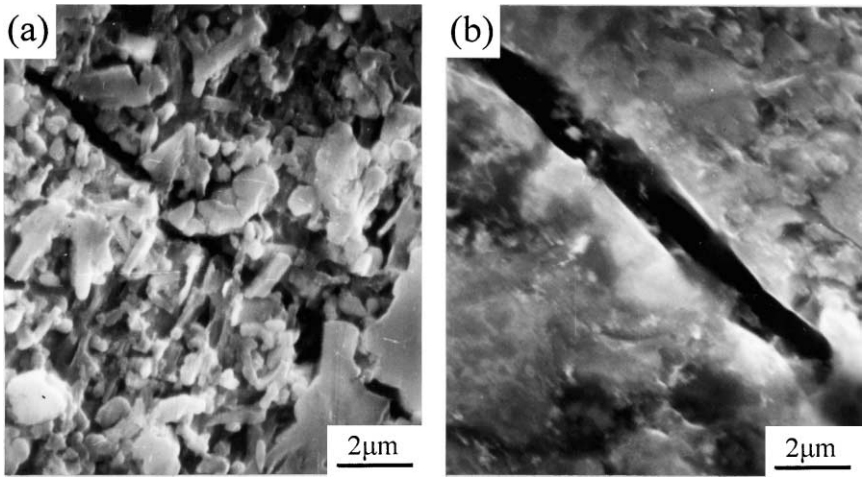

Fig. 13. Crack propagation produced by the Vickers indentation (a) 60 wt.% BAS composites in which bridging and crack deflection is obvious; (b) 100% BAS matrix in which no visible bridging and crack deflection can be observed.

presence of low-melting point compounds will cause intergranular sliding which result in the degradation of mechanical properties.

Fracture toughness of Si_3N_4/BAS composites at room temperature versus BAS content is displayed in Fig. 10. The toughnesses of the BAS matrices are very low (1.78 ± 0.20 MPa $m^{1/2}$). The in situ formed rod-like β-Si_3N_4 whiskers obviously increase the fracture toughness of the composites (the fracture toughness of 60 wt.% BAS composite reinforced with Si_3N_4 is 3.24 ± 0.42 MPa $m^{1/2}$). Table 3 also shows that the fracture toughness of the composites with longer sintering time and addition of BAS seeds tends to get higher values than the average one of the composite.

The interaction between the crack and the microstructure of the composites can be demonstrated clearly by examining the crack propagation produced by the Vickers indentation as shown in Fig. 13. In pure BAS matrix, the crack propagated directly through the matrix, resulting in a planar fracture path [Fig. 13(a)].

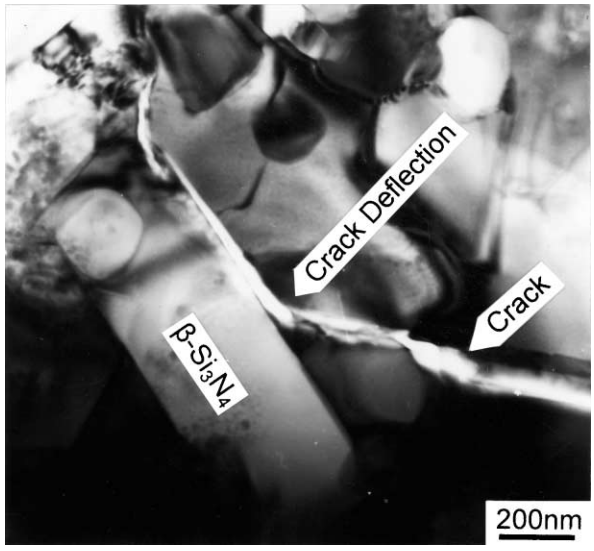

Fig. 14. Crack deflection in Si_3N_4/BAS composites under TEM observation, crack deflected and prolonged between the BAS–Si_3N_4 grain boundary.

In contrast, in 60 wt.% BAS composites, the propagating cracks tended to deflect along the Si_3N_4 whisker/matrix interface, and crack bridging and whisker debonding were commonly observed in the wake zone of the extending cracks [Fig. 13(b)]. This resulted in a more rough fracture path. Whisker pullout and bridging undoubtedly increased the fracture toughness of the composite, which is consistent with the mechanical property results. The crack shown in Fig. 14, which is induced by localized heating during TEM observation, follows a growing path along the whisker interface which shows contrast indications of dislocations and residual strain fields. The crack deflection and whisker-matrix interface debonding are evident. In either cases, the development of interface debonding allows the matrix crack to proceed without fracturing the whisker. Similar results have been observed in Refs. [4,5,14,21,22].

4. Conclusions

1. BAS glass-ceramic is beneficial to the $\alpha \rightarrow \beta$ phase transformation of Si_3N_4 at low sintering temperature (1450 °C) and short sintering time (30–60 min), approximately 27.0–61.6% β-Si_3N_4 are formed during sintering.
2. In Si_3N_4/BAS composites, the β-Si_3N_4 whiskers and matrix grains are bonded directly, no amorphous layers are found under conventional TEM observation. But the decrease of elevated temperature flexural strength indicate that there might exist thin amorphous layers in the grain boundary.
3. The flexural strength and fracture toughness values of BAS glass-ceramics can be effectively improved by the in situ grown rod-like β-Si_3N_4 whiskers. The main toughening mechanisms are crack deflection, whisker bridging and pullout.
4. The 40 wt.% BAS matrix composite shows good high temperature mechanical properties and the flexural strength of the 40 wt.% Si_3N_4/BAS composite at 1200 °C decreased only by 5.84% compared to the room temperature strength.

References

[1] C.H. Drummond, W.E. Lee, Crystallization of a barium aluminosilicate glass, Ceram. Eng. Sci. Proc. 10 (9–10) (1989) 1485–1502.
[2] E.J. Wuchina, I.G. Talmy, The effects of the presence of hexacelsian on the properties of celsian ceramics. Proceedings of the 14th Conference on Metal, Carbon and Ceramic Composites, NASA Conf. Publ. 3097 (1) (1990) 239–250.
[3] A.H. Lubis, N.L. Hecht, G.A. Graves Jr., R. Ruh, Microstructure–property relations of hot-pressed silicon carbide–aluminum nitride compositions at room and elevated temperature, J. Am. Ceram. Soc. 82 (9) (1999) 2481–2489.
[4] F. Ye, T.C. Lei, Y. Zhou, Interface structure and mechanical properties of Al_2O_3–20 vol.%SiCw ceramic matrix composite, Mater. Sci. Eng. A 281 (2000) 305–309.
[5] H.W. Jang, K.S. Kim, C.J. Jung, Development of SiC-whisker-reinforced lithium aluminosilicate matrix composites by a mixed colloidal processing route, J. Am. Ceram. Soc. 75 (10) (1992) 2883–2886.
[6] L.A. Xue, I.W. Chen, A new SiC-whisker-reinforced lithium-aluminosilicate composite, J. Am. Ceram. Soc. 76 (11) (1993) 2785–2789.
[7] J.J. Brennan, S.R. Natt, SiC-whisker-reinforced glass-ceramic composites: interfaces and properties, J. Am. Ceram. Soc. 75 (5) (1992) 1205–1216.
[8] K.P. Gadkaree, Whisker reinforcement of glass-ceramics, J. Mater. Sci. 26 (9) (1991) 4845–4854.
[9] K.P. Gadkaree, K. Chyung, Silicon-carbide-whisker-reinforced glass and glass-ceramic composites, Am. Ceram. Soc. Bull. 65 (2) (1986) 370–376.
[10] J.J. Brennan, K.M. Prewo, Silicon carbide fibre reinforced glass-ceramic matrix composites exhibiting high strength and toughness, J. Mater. Sci. 17 (1982) 2371–2383.
[11] J.D. Birchall, D.R. Stanly, M.J. Mockford, G.H. Pigott, P.J. Pinto, Toxicity of silicon carbide whiskers, J. Mater. Sci. Lett. 7 (1989) 350.
[12] A.J. Pyzik, D.R. Beaman, Microstructure and properties of self-reinforced silicon nitride, J. Am. Ceram. Soc. 76 (11) (1993) 2737–2744.
[13] K.M. Prewo, J.J. Brennan, Fiber reinforced glasses and glass-ceramics for high performance application, Am. Ceram. Soc. Bull. 65 (2) (1986) 305–313.
[14] T. Mah, M.G. Mendiratta, High-temperature mechanical behavior of fibre-reinforced glass-ceramic-matrix composites, J. Am. Ceram. Sci. 68 (9) (1985) 248–251.
[15] B. Zhang, L. Zhang, W. Zhou, Aqueous sol–gel route to barium aluminosilicate glass-ceramics, J. Am. Ceram. Soc. 82 (1) (1999) 253–256.
[16] F. Ye, Postdoctoral report (in Chinese), Northwestern Polytechnical University, China, 1997.
[17] C.P. Gazzara, D.R. Messier, Determination of phase content of Si_3N_4 by X-ray diffraction analysis, Am. Ceram. Soc. Bull. 56 (9) (1977) 777–780.
[18] D.W. Freitag, In situ processed Si_3N_4 whiskers in the system barium aluminosilicate–Si_3N_4, Mater. Sci. Eng. A 195 (1995) 7–205.
[19] S. Hampshire, Nitride ceramics, in: M.V. Swain (Ed.), Structure and Properties of Ceramics, Australia, 1998, Vol. 6, p. 150.
[20] A.E. Pasto, J.T. Neil, C.L. Quakenbush, in: L. Hench, D. Ulrich (Eds.), Ultrastructure Processing of Ceramics Glasses and Composites, Wiley, New York, 1984, pp. 476–489.
[21] F. Yu, C.R. Ortiz-Longo, K.W. White, The microstructure characterization of in situ grown Si_3N_4 whisher-reinforced barium aluminum silicate ceramic matrix composite, J. Mater. Sci. 34 (1999) 2821–2835.
[22] Y.-W. Kim, Y.-I. Lee, M. Mitomo, Fabrication and mechanical properties of silicon carbide–silicon nitride composites with oxynitride glass, J. Am. Ceram. Soc. 82 (4) (1999) 1058–1060.